MASTERARBEIT / MASTER'S THESIS

Titel der Masterarbeit / Title of the Master's Thesis

„Structural Preformation of the Intrinsically Disordered Protein Fragment YAP 50-171"

verfasst von / submitted by

Michael Feichtinger, BSc

angestrebter akademischer Grad / in partial fulfilment of the requirements for the degree of

Master of Science (MSc)

Wien, 2017 / Vienna 2017

Acknowledgements

I want to dedicate the first page of my thesis to people who supported me during the last few years of my studies and helped me reaching this first goal.

First, I would like to thank my supervisor Robert Konrat for the possibility to join his lab for my master thesis. I'm especially grateful for introducing me into the beauty of NMR spectroscopy and offering new points of view on proteins. The support you gave me brought back my strong interest into science and new perspectives to combine it with my other fields of interest.

Many thanks to all members of the amazing lab I am allowed to be part of. Especially to Tomas and Borja for their valuable scientific input and support with the experiments to carry out my master thesis. Thanks to Karin for maintaining the lab environment and my mental health in hours of despair. This place already became a second home for me and colleagues turned into friends.

A big "thank you" to my whole family; my wonderful sister Tina and my grandparents. Thank you for never losing your faith in me.

Franziska, your loving and creative nature is a limitless source of energy for me. I am very grateful for withstanding all my moods, spending so many years with me, permanently giving me new inputs, and embellishing my life.

Finally, I would like to thank my biggest supporters, my beloved parents Sandra and Michael. Without your endless support of my ambitions and interest, I would never have been able to write this thesis. Thank you.

Abstract

Intrinsically disordered proteins (IDPs) can carry out a whole plethora of biological functions and a growing interest in IDPs is particularly due to their central roles in protein interaction networks. Within these networks, IDPs often serve as central hubs as they can function as targets for different molecules due to their structural flexibility. In addition, several IDPs can also bind to the same target as they are able to adopt their structures. IDPs are implicated in a whole variety of human diseases, including cancer, neurodegenerative diseases, and diabetes. Hence, IDPs offer potential targets for therapeutic interventions. Furthermore, IDPs challenge traditional binary structured-unstructured descriptors.

A well-established method to study IDPs on an atomic level is Nuclear Magnetic Resonance (NMR) spectroscopy. NMR offers a multitude of determinable parameters to characterize IDPs, ranging from dynamic descriptors to long- and short-range indicators. NMR, therefore, enables the measurement of ensemble-averaged conformational parameters from the nuclei distributed throughout the protein.

Yes associated protein (YAP) is an IDP that plays a major role in the Hippo pathway, regulating organ size, cell proliferation, apoptosis, and it is associated with cancer development. Therefore, the binding between the YAP and TEA domain transcription factors (TEADs) is an interesting target for cancer therapy. The TEAD binding domain of YAP is mapped to the protein residues 50-171. The YAP binding domain of TEAD is mapped to the C-terminal fragment. Therefore, these fragments of the proteins are used for further research.

This thesis presents a first structural characterization of the intrinsically disordered protein fragment YAP 50-171 in the unbound state and new insights in the bound state. Structural preformation of the secondary structure elements, namely, a β-strand (residues 52-58), an α-helix (residues 61-73) and an Ω-loop (residues 86-100), and the tertiary structure of the bound state are shown. The evidence for structural preformation is achieved by the application of chemical shift analysis, determination of ^{15}N Relaxation parameters, the probing of short-range interactions by the measurement of Nuclear Overhauser Effects (NOEs), and long-range interactions by the measurement of paramagnetic relaxation enhancements (PREs). The binding mode of YAP to TEAD4 is suggested as mainly conformational selection. The previously known binding interface between YAP and TEAD4 is confirmed by a comparison of the HSQC spectra with different YAP:TEAD4 molar ratios. Nevertheless, the mapped binding site is slightly larger than its previous descriptions. Furthermore, two additional affected sites of YAP upon binding to TEAD4 are first described.

Zusammenfassung

Intrinsisch ungeordnete Proteine (IDPs) führen eine Fülle an biologischen Funktionen aus und das steigende Interesse, welche diesen in den letzten Jahren zugekommen ist, kommt vor allem daher, dass IDPs zentrale Rollen in Proteininteraktionsnetzwerken einnehmen. In diesen Netzwerken dienen IDPs oftmals als zentrale Schnittstelle, da sie auf Grund ihrer strukturellen Flexibilität von verschiedene Molekülen gebunden werden können. Zusätzlich können mehrere unterschiedliche IDPs auch an das gleiche Zielmolekül binden. IDPs sind außerdem in eine ganze Bandbreite an Krankheiten involviert, mitunter Krebs, neurodegenerative Erkrankungen und Diabetes. Deswegen bieten sich IDPs als potentielle Ziele für therapeutische Interventionen an. Weiters stellen IDPs klassische binäre Unterscheidungen, wie strukturiert und unstrukturiert, in Frage.

Eine etablierte Methode zur Untersuchung von IDPs auf atomarer Ebene bietet die Kernspinresonanzspektroskopie (NMR). NMR ermöglicht die Bestimmung einer Vielzahl an Parametern zur Charakterisierung von IDPs. Diese reichen von dynamischen Deskriptoren bis hin zu Parametern für kurz- und weitreichende Interaktionen. Damit ist es durch NMR Spektroskopie möglich einen Ensemble-Durchschnitt konformativer Parameter der Atomkerne von Proteinen zu messen.

Yes assoziiertes Protein (YAP) ist ein IDP und nimmt eine zentrale Rolle in der Hippo Signaltransduktion ein, welche Organgröße, Zellproliferation und Apoptose reguliert. Weiters ist YAP mit der Entstehung von Krebs assoziiert. Deswegen bietet sich die Binding zwischen YAP und den TEA Domänen Transkriptionsfaktoren (TEADs) als ein interessantes Ziel für die Krebstherapie an. Die TEAD-Bindungsdomäne von YAP wurde zwischen den Aminosäuren 50 und 171 von YAP beschrieben. Die YAP-Bindungsdomäne von TEAD wurde am C-terminalen Fragment entdeckt. Deswegen wurden in der folgenden Studie diese Proteinfragmente verwendet.

Diese Masterarbeit präsentiert eine erste strukturelle Charakterisierung des intrinsisch ungeordneten Protein Fragments YAP 50-171 im ungebunden Zustand und bietet außerdem neue Einsichten in den gebundenen Zustand and TEAD4. Es wird gezeigt, wie sowohl Sekundärstrukturelemente, im Detail ein β-Strang (52-58), eine α-Helix (61-73) und ein Ω-Loop (86-100), als auch die Tertiärstruktur bereits im ungebunden Zustand vorgeformt ist. Dies wird erreicht mittels der Anwendung einer Analyse der chemischen Verschiebungen, der Bestimmung von ^{15}N Relaxationsparametern, der Erforschung von kurzreichenden Interak-

tionen mittels der Messung von Kern-Overhauser-Effekten (NOEs) und weitreichender Interaktionen mittels der Messung von paramagnetischen Relaxationsverstärkung (PREs). Als Bindungsmodell zwischen YAP und TEAD und wird deswegen konformative Selektion vorgeschlagen. Die zuvor bekannte Interaktionsstelle zwischen YAP und TEAD4 wird mittels des Vergleiches von HSQC Spektren mit unterschiedlichen molaren Verhältnissen von YAP und TEAD4 bestimmt. Nichtdestrotzt ist die hier beschriebene Bindungsstelle etwas größer. Außerdem werden noch zwei zusätzliche Teile von YAP beschrieben, welche durch die Bindung an TEAD4 beeinträchtigt werden.

Table of Content

1 Introduction

All living organisms consist of similar building blocks (lipids, carbohydrates, DNA, RNA, proteins, etc.) arranged in an organized way. A major component is protein, which can carry out a multitude of functions; one of these functions is signal transmission via binding to another protein. So far, two different models detailing how this binding occurs has been described, namely conformational selection and induced fit. Both of these models build on the idea of a static lock-and-key model for protein interaction, which was described over a century ago (Fischer 1894). According to the induced fit model, the structure of the targeted protein adopts on binding. (Koshland 1958). In contrast, in the case of conformational selection, the binding molecule selects a certain conformational state of the substrate thereby shifting the equilibrium between the different conformational states towards the preferred state (Tsai et al. 1999). Nevertheless, many binding events are a combination of both models (Hammes et al. 2009).

In the second half of the last century, a common sense prevailed in structural biology which dictated that a fixed structure was the prerequisite for function. With the beginning of the new millennium, the intrinsically disordered proteins (IDPs) were recognized to fulfill a broad range of biological functions without possessing a single fixed structure (Tompa 2011; Oldfield and Dunker 2014) thereby questioning the traditional structure function paradigm (Wright and Dyson 1999). Since then, there has been rapid growth in the field of studying IDPs, involving an increasing number of publications (Uversky 2014). Owing to their lack of structural constraints, IDPs can carry out a whole plethora of biological functions and an interest in them is especially due to their central roles in protein interaction networks (Dunker et al. 2005). Within these networks, IDPs often serve as central hubs as they can function as targets for different molecules due to their structural flexibility. In addition, several IDPs also can bind to the same target as they are able to adopt their structures (Oldfield and Dunker 2014). IDPs are implicated in a whole variety of human diseases, including cancer, neurodegenerative diseases, and diabetes. Hence, IDPs offer potential targets for therapeutic interventions (Iakoucheva et al. 2002; Metallo 2010; Uversky 2011; Zhang et al. 2015). Furthermore, IDPs challenge the binary order-disorder and structured-unstructured descriptors as they exist in dynamic conformational ensembles with different degrees of order and disorder (Konrat 2015).

The inherent structural flexibility of IDPs mandates the use of new experimental methods without the restrictions of X-ray crystallography, which is one of the most successful methods applied in structural biology. Nevertheless, X-ray crystallography cannot describe the heterogeneous structural ensembles of protein molecules. A well-established method to study IDPs on an atomic level is Nuclear Magnetic Resonance (NMR) spectroscopy. NMR offers a multitude of determinable parameters to characterize IDPs, ranging from dynamic descriptors to long- and short-range indicators (Konrat 2014). NMR, therefore, enables the measurement of ensemble-averaged conformational parameters from nuclei distributed throughout the protein (Jensen et al. 2013). The properties of NMR spectroscopy and the fact that the NMR signals of IDPs exhibit the spectroscopic features of small molecules, therefore, offers a great combination to investigate these dynamic systems. The system characterized in this work by NMR spectroscopy is the intrinsically disordered protein fragment Yes-associated protein (YAP) 50-171.

YAP is an partly intrinsically disordered protein transcribed into four different isoforms ranging from 326 to 504 residues (Santucci et al. 2015). YAP is a major target and a terminal effector of the Hippo pathway. The Hippo pathway was first discovered through genetic screens in *Drosophila*, in which it regulates cell growth (Halder and Johnson 2011; Staley and Irvine 2012); it was shown that the Hippo pathway conserved among other animals. In mammals, the Hippo pathway regulates organ size, cell differentiation, and regeneration (Zhao et al. 2011; Tremblay and Camargo 2012). Furthermore, the deregulation of the Hippo pathway is associated with cancer development (Liu et al. 2012; Pobbati and Hong 2013; Ma et al. 2015; Pobbati et al. 2015).

One of the functions of YAP is to bind the TEA domain transcription factors (TEADs) as a transcriptional coactivator. Four closely related TEADs in humans are known: TEAD 1-4. All four TEADs possess an N-terminal domain that binds to DNA, and mediates transcription and a C-terminal YAP binding domain. Together, YAP and TEAD form a functional heterodimeric transcription complex that activates the expression of Hippo-responsive genes (Pobbati and Hong 2013; Pobbati et al. 2015). Therefore, the YAP:TEAD interaction might be a promising therapeutic approach in cancers where the Hippo pathway is deregulated. The formation of the YAP:TEAD complex is indirectly regulated by YAP phosphorylation, which prohibits the nuclear translocation of YAP and leads to the downregulation of genes

related to proliferation, therefore, leading to apoptosis (Zhao et al. 2007). The phosphorylation of YAP is a result of the activation of the core kinase cassette of the Hippo pathway and occurs in the cytoplasm. Thus, phosphorylation at S127 leads to cytoplasmic retention via binding to 14-3-3 proteins (Zhao et al. 2007); in addition, phosphorylation at S381 primes YAP for further phosphorylation events that induce degradation (Zhao et al. 2010).

Previously, the TEAD binding domain of YAP was mapped to the protein region 50-171 (Vassilev et al. 2001). Furthermore, the crystal structure of YAP 50-171 and TEAD1 194-411 (corresponding to the C-terminal YAP binding domain) was solved, but the residues 101-171 had no electron density and were not built into the model (Li et al. 2010). However, the affinities of the different YAP fragments of protein region 50-171 were determined. They showed the irreducibility of the TEAD binding domain to a smaller protein fragment of YAP. They reported a significant decrease of the dissociation constant (K_d) for YAP 50-99 in comparison to YAP 50-171 (Hau et al. 2013).

Fig. 1-1: Crystal structure of YAP 50-171 (red) and TEAD1 194-411 (green). The YAP region 101-171 possessed no electron density and is missing in the model (Li et al. 2010).

The crystal structure (see Fig. 1-1) revealed three binding interfaces between YAP and TEAD: a β-strand (residues 52-58), an α-helix (residues 61-73) and an Ω-loop (residues 86-100) (Li et al. 2010). Furthermore, key residues in the binding site and their contribution to the binding have been described (Mesrouze et al. 2017). It was shown that the mutation of

certain hydrophobic residues in the α-helix and Ω-loop strongly affect binding affinities. The strongest effects (ΔΔG > 4 kcal/mol) were generated with mutations of R89, L91, and F95. These findings were in agreement with earlier works showing the importance of some of these residues (Zhang et al. 2014).

Nevertheless, all the studies carried out so far have mainly focused on the bound state of YAP to TEAD, mainly due to the insufficiency of the applied methods for characterizing the intrinsically disordered protein fragment in the free form on an atomic level. Therefore, this thesis reports new structural insights into the unbound and bound state of YAP 50-171 via NMR spectroscopic methods.

2   Results

2.1 ^{1}H, ^{13}C, ^{15}N Resonance Assignment and Chemical Shift Analysis

The first step to get atom-specific information about a protein with NMR is the ^{1}H, ^{13}C, ^{15}N resonance assignment. Typically, triple-resonance experiments are carried out to find sequential connectivity between neighboring residues. This strategy relies on coherence transfer steps on the backbone ^{1}H, ^{13}C, ^{15}N atoms (Konrat 2014). The backbone assignments of YAP were obtained using BEST-TROSY type versions of HNCANNH, HN(COCA)NNH, HNCACB, HN(CO)CACB, HNCO, and HN(CA)CO experiments (Solyom et al. 2013).

Fig. 2-1: (A) 1H-15N TROSY HSQC spectrum of YAP 50-171 at pH 6 and 298 K. (B) Magnification of the central region of the spectrum.

Assignment of the backbone amides ^{1}H, ^{15}N of YAP 50-171 is shown in Fig. 2-1. The spectrum shown is the ^{1}H-^{15}N HSQC, the most standard and utilized experiment in protein NMR. It shows all the H-N correlations. These are mainly the backbone amide groups, but Asparagine, Glutamine, and Tryptophan side chains, which contain NH groups, are also visible (Cavanagh et al. 2007).

Backbone amide resonances were assigned for all the 108 non-Proline residues, except of K76, K90, K97, K102, H104, and H126. In addition, 94% of the Cα and Cβ resonances of the respective residues and 81% of C' resonances were assigned. The two missing Histidine peaks are a result of exchange broadening, because the measurements were carried out at pH 6 and, therefore, close to the side chain pK_a of Histidine. Presently, there is no feasible explanation for the missing Lysine peaks. An intact mass analysis of the protein by mass spectrometry showed that the mass is correct for the supposed protein sequence (see Fig. 2-2).

50	60	70	
AGHQIVHVRG	DSETDLEALF	NAVMNPKTAN	
80	90	100	
VPQTVPMRLR	KLPDSFFKPP	EPKSHSRQAS	
110	120	130	
TDAGTAGALT	PQHVRAHSSP	ASLQLGAVSP	
140	150	160	170
GTLTPTGVVS	GPAATPTAQH	LRQSSFEIPD	DV

Fig. 2-2: Protein sequence of YAP 50-171.

Backbone chemical shifts depict favorable data for the analysis of local and overall structural propensities. Deviations of the chemical shifts from chemical shifts in theoretical random coils can, in particular, be used to predict secondary structure propensities (Kjaergaard and Poulsen 2012). For determining the overall tendencies of proteins populating a more folded or unfolded state, the dispersion of the peaks in the ^{1}H dimension of the ^{1}H-^{15}N HSQC spectrum are utilized. The very narrow peak dispersion in the ^{1}H dimension of the HSQC spectrum of YAP shows that YAP 50-171 is intrinsically disordered. Nevertheless, the secondary

structure propensity (SSP) score (Marsh et al. 2006) clearly indicates a propensity for a pre-formed α-helix in the unbound state (Fig. 2-3). Furthermore, the protein seems to preferentially adopt extended structures (negative SSP scores).
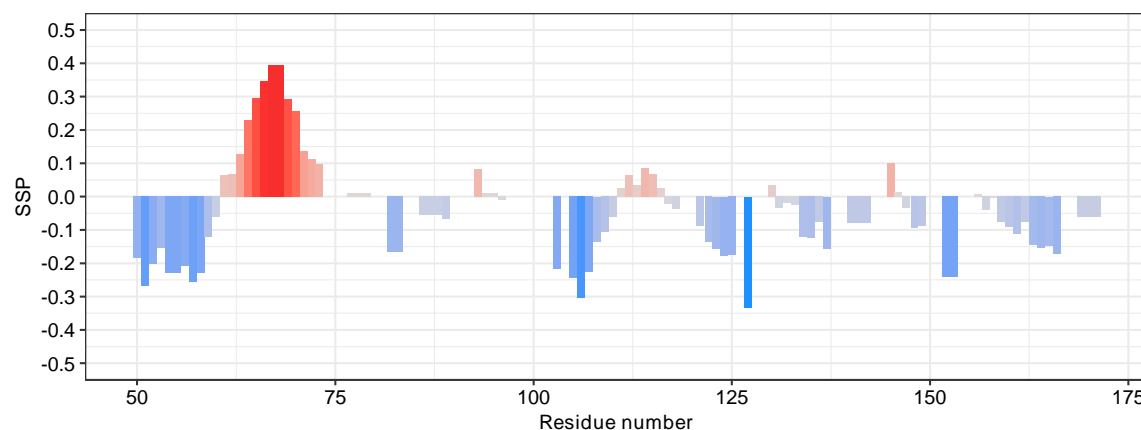

Fig. 2-3: SSP score (Marsh et al. 2006) of YAP 50-171 at pH 6 and 298 K. Positive scores indicate a propensity for α-helical structures, whereas β-strands or extended structural elements possess a negative score.

2.2 ^{15}N Relaxation Data

NMR relaxation data of proteins in solution contain information on the internal motions that occur in a system. These relaxation data are linked to local and global dynamics of the protein (Lipari and Szabo 1982). The two relaxation phenomena measured here are spin-lattice and spin-spin relaxation. Spin-lattice relaxation (characterized by the time constant T_1 or the relaxation rate R_1) refers to the restoration of the Boltzmann distribution of spins and results from coupling of excited spins with their environment. Spin-spin relaxation (characterized by the time constant T_2 or the relaxation rate R_2) refers to the loss of coherence between spins as there are individual variations in the Larmor frequency of spins, resulting from fluctuations in their local magnetic fields. The heteronuclear nuclear Overhauser effect (NOE) is dependent on the dipole-dipole distance and the gyromagnetic ratio of each spin (Cavanagh et al. 2007; Levitt 2008; Reddy and Rainey 2010).

R_1 and R_2 relaxation rates, in combination with the ^{1}H-^{15}N heteronuclear NOEs, are utilized to characterize the backbone dynamics of IDPs. All the three parameters are sensitive to the motions in the picosecond to the nanosecond timescale, but heteronuclear NOEs are most sensitive for the high-frequency motions of the protein backbone. R_2 rates are the most informative on microsecond to millisecond motions and conformational exchange processes,

whereas R_1 rates contain information on motions occurring on a millisecond to second time-scale. An analysis of the relaxation data is useful for characterizing structural preferences and secondary structure elements (Tompa 2010). In general, regions adopting secondary structures are expected to show slower dynamics than completely unstructured regions. Furthermore, heteronuclear NOEs are sensitive to local mobility, whereupon reduced NOEs (larger values) indicate restrictions in the local mobility. Increased R_2 rates are indicators of secondary structure formation (Danielsson et al. 2008).
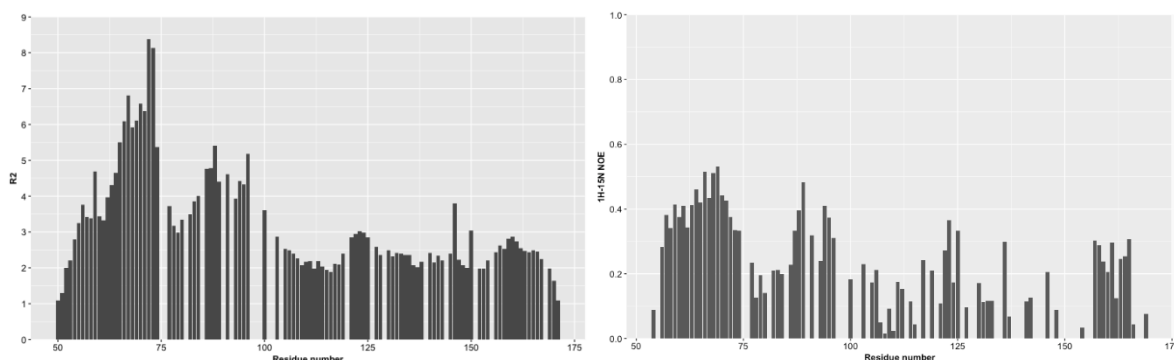
2.2.1 R_2 Rates and Heteronuclear ^{1}H-^{15}N NOEs

Fig. 2-4: R_2 and ^{1}H-^{15}N heteronuclear NOE data of YAP 50-171 at pH 6 and 298K. Increased R_2 rates indicate secondary structure formation and larger NOE values indicate restricted mobility. Large negative NOE values for the very N- and C-terminal residues of the protein are not shown in the plot.

The R_2 and the heteronuclear ^{1}H-^{15}N NOE data (see Fig. 2-4) of YAP show a significant indication for structure formation and restricted mobility in the protein region between the residues 50 and 100. This region is the visible part in the crystal structure of the bound state of YAP (see Fig. 1-1). Notably, the region between L65 and N74 shows the highest R_2 rates. This region corresponds to the α-helical region in the crystal structure. Furthermore, the consequent linking region between the α-helix and the Ω-loop exhibits significantly lower R_2 rates and NOE values. Within the Ω-loop region, a decrease in the motional restriction is visible in the more flexible region between L91 and D93. In contrast, the residues promoting the lower of the Ω-shape and, therefore, creating the specific structural motif exhibit higher R_2 and NOE values. In addition, the two regions spanning from A117 to A125 and from A157 to S163 show increased R_2 rates and NOE values.

2.2.2 Characterizing Anomalous R_2 Rates

As mentioned above, R_2 rates are also informative for exchange events. In comparison to the surrounding residues, V72 and M73 show significantly higher R_2 rates. One way to identify

the residues undergoing chemical exchange is through the ratio R_2/R_1 (Kay et al. 1989). Nevertheless, this approach is not able to discriminate between motional anisotropy and chemical exchange. This can be achieved by a combinatorial analysis of R_2/R_1 versus R_1R_2 (Kneller et al. 2002). Applying this analysis on YAP indicates that V72 and M73 (see top right of Fig. 2-5) undergo chemical exchange.
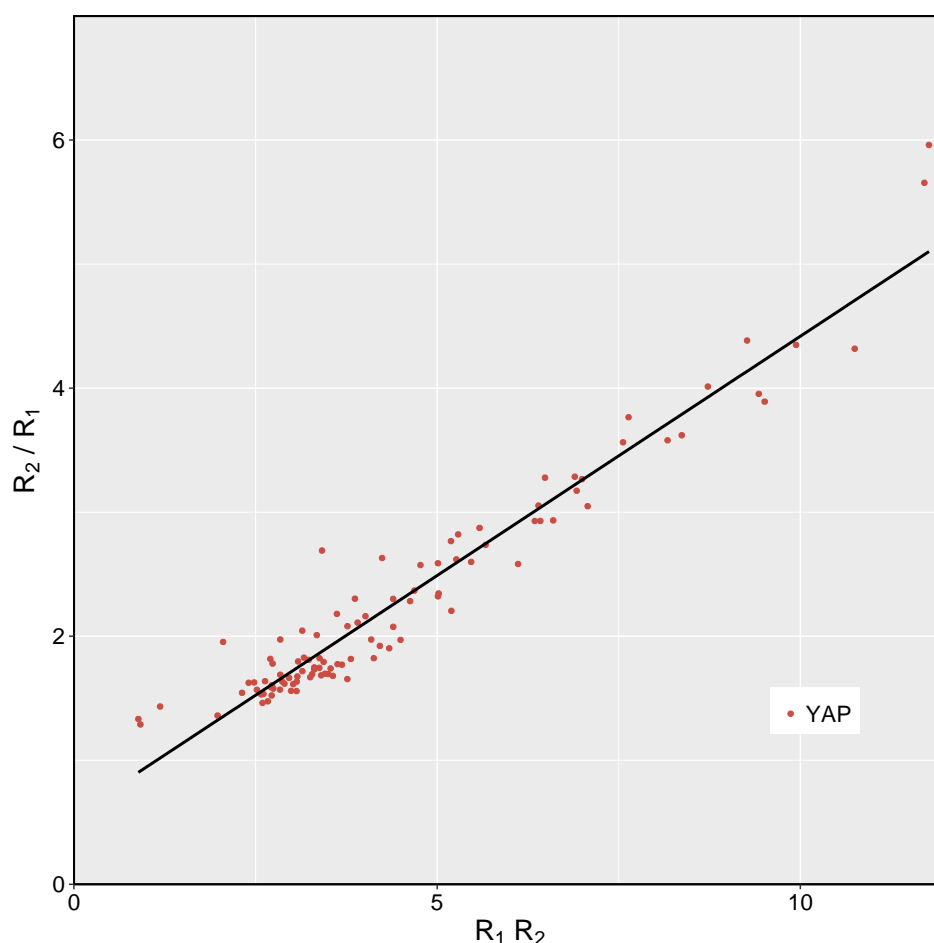

Fig. 2-5: R_2/R_1 versus R_1R_2 plot of YAP 50-171 at pH 6 and 298 K. This plot enables one to identify the residues undergoing chemical exchange and excluding motional anisotropy.

To further investigate this slow dynamic phenomenon, a CPMG dispersion experiment with constant relaxation time (Tollinger et al. 2001) was carried out. Conformational exchange in a residue modulates the chemical shift of the effected residue. Hence, the effective transverse relaxation rate (R_2) is affected if exchange events take place.

Plotting ΔR_2 between the spectrum with the lowest number of CPMG pulses and the one with the highest number of CPMG pulses offers the first hints on affected residues (see Fig. 2-6A). Beside the two other residues, the plot indicates that V72 and M73 undergo chemical exchange. In addition, the CPMG profiles of V72 (see Fig. 2-6B) and M73 (see Fig. 2-6C)

support these assumptions. In addition, the residues T77 and A78, which are close to V72 and M73, show higher ΔR_2 rates as well.
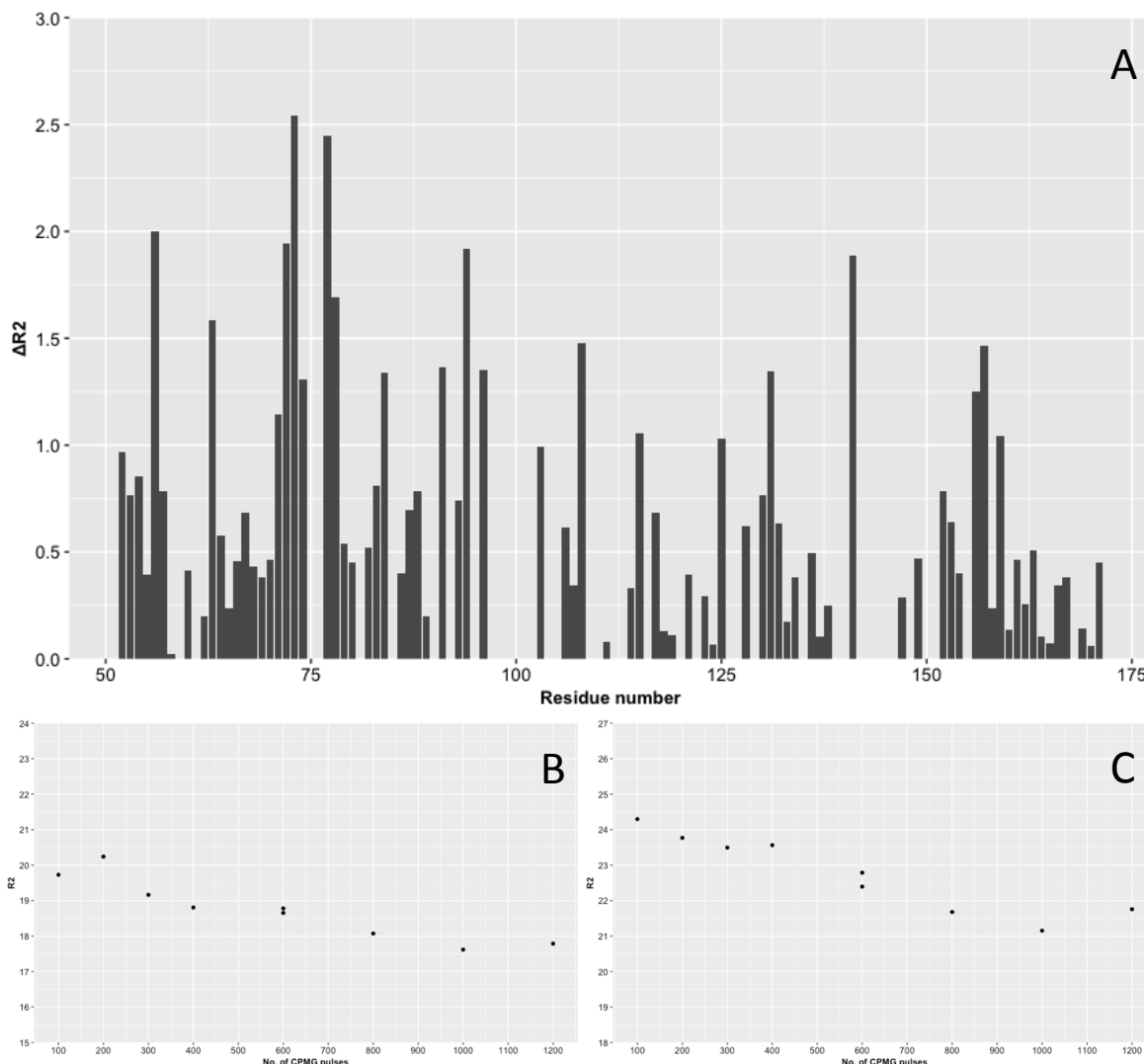

Fig. 2-6: (A) ΔR_2 between the spectrum with the lowest number of CPMG pulses and the one with the highest number of CPMG pulses of YAP 50-171 at pH 6 and 298 K; (B) The effective transverse relaxation rate R_2, as a function of CPMG pulses for V72; and (C) M73.

2.3 Paramagnetic Relaxation Enhancement (PRE)

The distance limit for ^{1}H-^{1}H NOEs (see section 2.4) of about 6 Å makes it an insufficient parameter to characterize long distance interactions. Therefore, a well-established method to identify and characterize transient long-range interactions in IDPs is the measurement of paramagnetic relaxation enhancements (PREs) (Konrat 2014). The basic principle of this application is the introduction of a paramagnetic spin label, usually a compound that contains

a nitroxide free radical that increases the relaxation rates of nearby nuclei in a distance-related manner (Kosen 1989). The alteration of the transverse relaxation depends on the inverse sixth power of the distance ($1/r^6$). This enables one to detect interactions between the unpaired electron and protons up to 35 Å (Clore 2015).

2.3.1   PRE Mutation Site Selection

The spin label chosen for YAP is MTSL, which is introduced into the protein by covalently attaching it to the thiol group of a Cysteine. The sequence of YAP 50-171 contains no Cysteines; therefore, they have been introduced into the sequence by site-directed mutagenesis. The choice of the mutation/labeling site is not trivial without the prior knowledge of compact structural elements within the protein as the introduction of spin labels/mutations at crucial sites will perturb the structure (Konrat 2014). Hence, the sequence-based protein meta-structure approach (Konrat 2009) was applied to predict the compact areas of the protein structure and choose three mutation sites distributed over the 121 amino acid proteins in areas of low compactness (see Fig. 2-7). Owing to the size of YAP, three mutation sites are sufficient to cover the whole protein. Therefore, one mutant with an N-terminal (-1C) Cysteine, one mutant with a Cysteine in the middle (S103 to C103), and one mutant with a C-terminal (172C) Cysteine were produced. Curiously, the insertion of a Cysteine at the N-terminus of the protein sequence dramatically altered the expression properties and protein stability. Therefore, all the data measured on the unstable -1C mutant have been excluded.
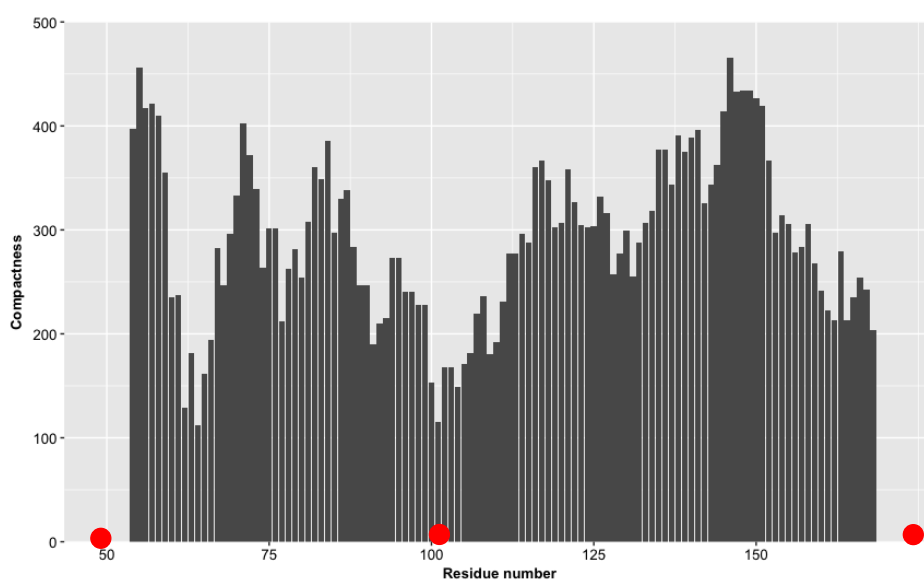

Fig. 2-7: Compactness per residue of YAP 50-171 predicted by the sequence-based protein meta-structure approach (Konrat 2009). The red dots indicate the chosen Cysteine mutation sites at positions -1, S103, and 172.

2.3.2 PRE Profiles

Instead of using a simplistic approach to compare the peak intensities between the paramagnetic and diamagnetic correlation spectra and only obtain a ratio, the far more accurate transverse PRE rate Γ (Clore 2015) was determined. Γ rates represent the difference between the transverse relaxation rate R_2 of ^1H in the paramagnetic sample and in the diamagnetic control. For a completely disordered protein (in theory), one would expect high Γ values close to the spin label and fast decaying $(1/r^6)$ rates the further away the residue position is from the spin label site.
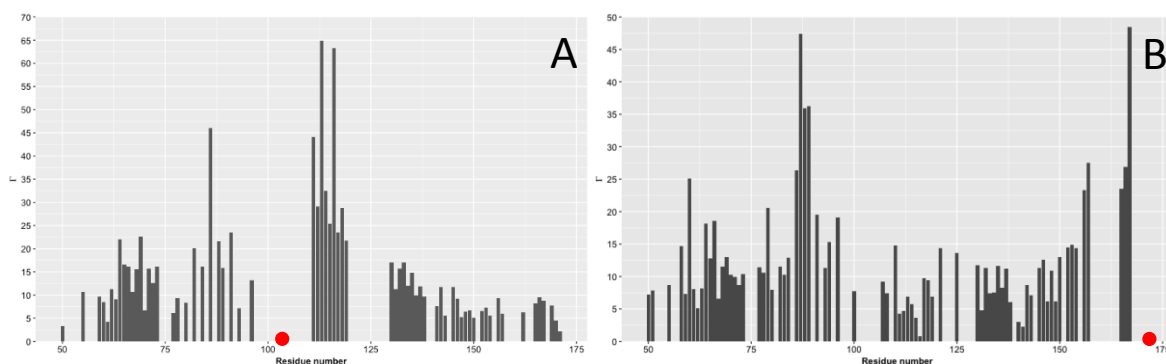

Fig. 2-8: Γ rates as a function of the residue position of YAP 50-171 mutants (1) 103C and (2) 172C at pH 6 and 298 K. The red dots indicate the the site of the spin label.

The PRE profiles of the YAP mutant 103C (see Fig. 2-8A) and 172C (see Fig. 2-8A) both indicate the population of a certain spatial arrangement. The 103C mutant shows a strong PRE around M86, part of the Ω-loop region, and an additional PRE between D64 and F69, the α-helical region. The Γ rates for the side of the Ω-loop region close to the spin label site are missing due to the proximity of this Ω-loop region to the spin label site and the Γ rates of the residues depicting the upper part of the Ω-shape in the Ω-loop are, in contrast, lowered, indicating its orientation away from the spin label site. The profile of the 172C mutant exhibits two similar PREs. Nevertheless, there is a very prominent PRE around R87, which is in the middle of the Ω-loop. Furthermore, there are increased PREs for the region between D60 and F69, i.e., the α-helical region. The protein region between the α-helix and the Ω-loop, N74 to V84, shows significantly lower PRE rates. Therefore, the PRE profiles indicate a spatial proximity of these two regions (α-helix and Ω-loop) and the spin label site.

2.4 ^{15}N-NOESY-HSQC

While the measurement of the PREs offers information about long range interactions, the measurement of NOEs is suitable to derive information on local transient structures in IDPs (Tompa 2010). The classical ^{1}H-^{1}H NOESY experiment, used for the early structure determination of small proteins, is based on the coherence transfer between ^{1}H nuclei to determine the distance constraints between them (Cavanagh et al. 2007). The signal overlap in the 2D NOESY made it inapplicable for (folded) proteins larger than 100 residues and mandated the development of the 3D methods (Zuiderweg and Fesik 1989). Furthermore, IDPs exhibit a very narrow peak dispersion in the ^{1}H dimension; therefore, the classical approach is even less convenient for IDPs. The advantage of using a ^{15}N-NOESY-HSQC is that ^{1}H-^{1}H correlations involving HN protons are related to the shift of the directly bonded ^{15}N. Therefore, one observes a separation of the classical NOESY along a third ^{15}N dimension (Marion et al. 1989).

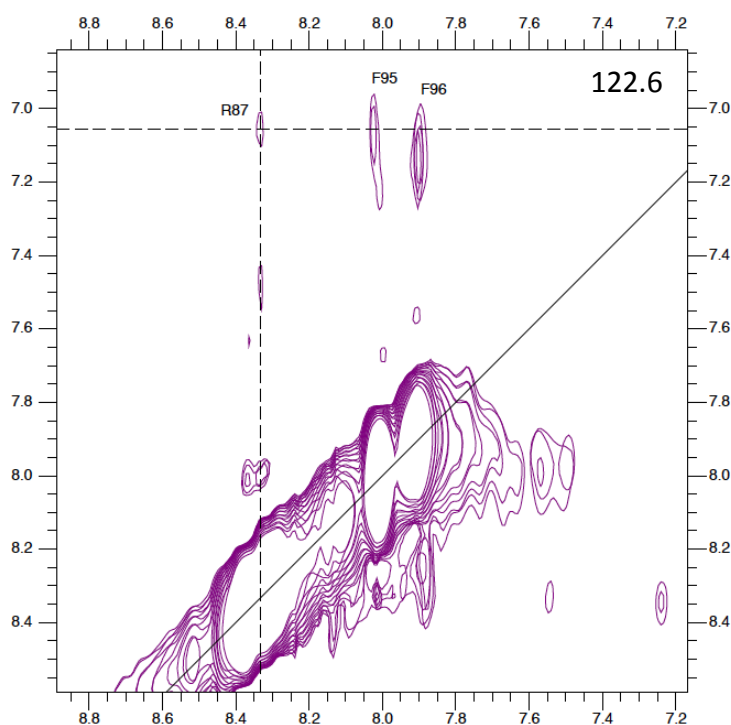
Fig. 2-9: Downfield region of ^{15}N-NOESY-HSQC of YAP 50-171 at pH 6 and 298 K showing the NOE between the amide proton of R87 and the aromatic ring of F95 (or F96). The ^{15}N frequency is indicated on the top right corner.

The application of the ^{15}N-NOESY-HSQC on YAP revealed that NOEs to the neighboring amides are only visible in regions of the protein with a higher degree of local order. They are strongly pronounced between E62 and V72, which correspond to the α-helical region.

Furthermore, residues in the Ω-loop region, between M86 and E100, exhibit NOEs between the neighboring HN protons. In addition, an NOE between the amide proton of R87 and the aromatic ring of F95 (or F96) appears in the spectrum (see Fig. 2-9). These residues are located on the opposing sites of the Ω-loop.

2.5   YAP:TEAD4 Binding

The first experiment to further characterize the binding between the two proteins with NMR spectroscopy is usually a titration of the binding partner. Therefore, the HSQC experiment is useful for detecting interactions with other proteins, because a change in relaxation due to the interaction affects the peaks of the residues that are directly involved. These peaks shift or even disappear from the spectrum (Tompa 2010). Therefore, HSQC spectra were recorded for ^{15}N labeled YAP and unlabeled TEAD4 with four different molar ratios with increasing amounts of TEAD4 and a stable amount of YAP (1:50, 1:10, 1:2, and 1:1).
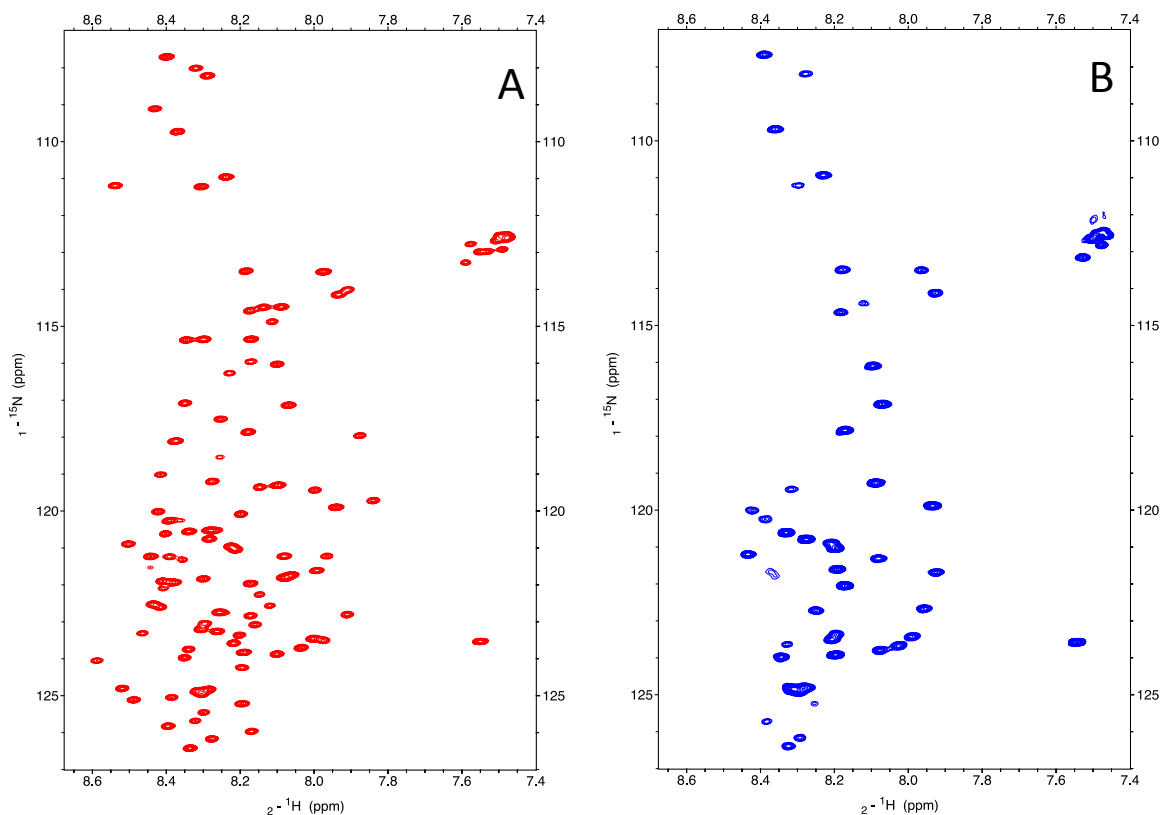

Fig. 2-10: HSQC spectra of YAP at pH 6 and 298 K in (A) apo state and (B) in a 1:1 molar ratio mixed with TEAD4.

The spectrum of YAP changed significantly between the apo and the 1:1 state (see Fig. 2-10). All the peaks for between A50 and R106 disappeared upon binding. In addition, the two sites of the protein are affected by the binding and show significant changes in the chemical

23

shifts of the residues with increasing amounts of TEAD4. The first site that exhibits changes is located between V123 and S128 (see Fig. 2-11A). In this region, all the residues except A125 disappear completely at a ratio of 1:1 between YAP and TEAD4. A125 exhibits lowered intensity in the final HSQC spectrum. The second region affected by the binding with TEAD4 is the C-terminal region between Q158 and F165 (see Fig. 2-11B-D).
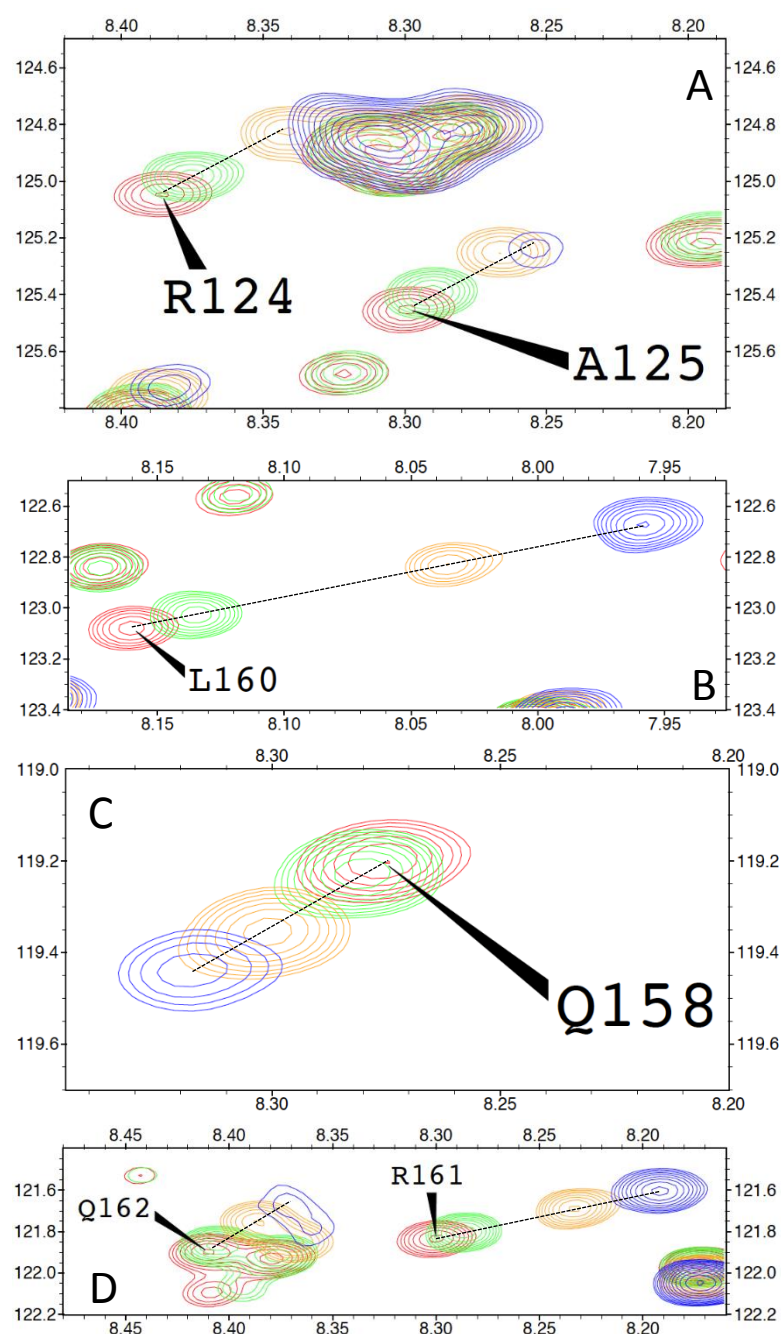

Fig. 2-11: Magnifications of the specific areas of the overlayed HSQCs for YAP at pH 6 and 298 K. Chemical shifts move along the trajectories (black dotted lines) from the apo state (red) with increasing molar ratios of TEAD4:YAP, namely 1:10 (green), 1:2 (orange), and 1:1 (blue).

3   Discussion

This thesis presents a first structural characterization of the intrinsically disordered protein fragment YAP 50-171 in the unbound state and new insights into the bound state. It is carried out by NMR spectroscopy. This thesis shows straightforward evidence that YAP exhibits preformation of secondary structure elements and a tertiary structure, even in the absence of a binding partner.

The SSP scores (Marsh et al. 2006), calculated from the chemical shifts obtained from the resonance assignment, already support the hypothesis of a preformed α-helix as described in the crystal structure (Li et al. 2010). Furthermore, the preformation of the β-strand in the beginning of the protein sequence is also indicated by the SSP scores. Nevertheless, the preformation of the β-strand is not as clear as with the α-helix and one has to be aware that the β-strand is located at the very N-terminus of the protein fragment used and this can affect the measured data. Further supporting data for the preformed α-helix are the R_2 rates and te heteronuclear NOEs. Both parameters show significantly increased values for this protein region. In addition, the backbone HN protons of the α-helical region possess clear NOEs to the protons of the neighboring amides. These NOEs are missing for most of the residual protein, thereby supporting their significance.

The preformation of the Ω-loop region of YAP is indicated by the increased R_2 rates and NOE values. Furthermore, the PREs of the YAP 103C mutant grant further support for this claim. The different PRE rates for the upper and the lower part of the Ω-loop falsify the assumption that this region is an extended and unstructured protein chain. Nevertheless, the strongest findings supporting the Ω-loop preformation are the ^{15}N-NOESY-HSQC data. Aside from the NOEs between the backbone HN protons in this region, the NOE between the amide proton of R87 and the aromatic ring of F95 (or F96) is a clear indicator that these residues are close together in space. Furthermore, previous binding studies (Mesrouze et al. 2017) have identified these residues as crucial contributors to the YAP:TEAD4 binding. In addition, one has to take into account that the ^{15}N-NOESY-HSQC has been recorded on a 500 MHz spectrometer. To further verify this finding, the measurement should be carried out on a spectrometer with a higher field strength. In addition, a specific ^{13}C labeling of the Phenylalanine's aromatic ring (Lichtenecker et al. 2013) in combination with a ^{13}C-NOESY-

HSQC (Cavanagh et al. 2007) can be used as an additional control experiment to detect the NOE of the backbone amide in the aromatic ring.

Residues 50 to 100 of YAP exhibit an L-shaped tertiary structure in the crystal structure (see Fig. 1-1). This part of YAP has significantly increased the R_2 rates and the NOE values in comparison to the more flexible part that is not visible in the crystal structure. Motional restriction in this larger part of the protein is an indicator for the preformation of a tertiary structure in this region. The PRE profiles further reveal that the spatial arrangement of the preformed secondary structure elements is already similar to the bound state. If this is the case, then the binding mode for YAP to TEAD4 comprises mainly conformational selection. To further test this hypothesis, one might measure the PREs of the bound state. As this is not possible with the current protein fragment of YAP, due to the disappearance of nearly half of the peaks on binding, one might work with a truncated version for further evaluation.

The exchange events taking place, foremost, in the protein region between V72 and A78 are additional indicators for the prevalence of this binding mode. The exchange that V72 and M73 undergo are, next to the CPMG data, backed up by the R_2/R_1 versus R_1R_2 analysis (Kneller et al. 2002). The potential causes for this exchange are either the C-terminal end of the α-helix changing between two states or the cis-trans-isomerization of the neighboring P75. Nevertheless, the conditions for the CPMG measurement need optimization and have to be carried out on different field strengths to quantify the exchange event. Furthermore, a CPMG measurement of the YAP 50-171 fragment with TEAD4, to check whether the exchange disappears upon binding, is not sufficient due to the disappearance of the peaks of interest. Therefore, a truncated version of YAP might be necessary.

The HSQC measurements of the YAP:TEAD4 complex confirm the binding site described in the crystal structure, but these previous findings might be incomplete. In addition to the residues 50 to 100, six succeeding residues of the YAP disappear on binding. Furthermore, two additional affected sites in the more flexible part of the YAP are revealed. In addition to the chemical shifts observed in these two sites, both show increased R_2 rates and NOE values in comparison to the surrounding regions in the unbound state. Hence, one can reject the claim that the shifts there are just artifacts. Their role in the binding cannot be determined with the current data and needs further investigation. Nevertheless, the contribution of the protein fragment 101-171 to the binding between YAP and TEAD4 has been previously

reported (Hau et al. 2013). Interestingly, the affected site from V123 to S128 overlaps with the described 14-3-3 binding site of YAP, whereas YAP gets phosphorylated at S127 to initiate this binding event (Zhao et al. 2007); it has, however, not been described any relation between this site and the TEAD binding. Measuring the YAP mutants 103C and 172C in the bound form, and determining ^{15}N relaxation parameters of the bound state might reveal further insights into the two affected sites initially described in this thesis.

In addition to the new insights gained about the IDP fragment YAP 50-171, this study points out that IDPs, like YAP, are challenging the predominating binary descriptor structured-unstructured. YAP appears as a conformational ensemble with different degrees of order and disorder. Therefore, it seems distorting to classify YAP as a disordered or unstructured protein. In the end, IDPs are proteins that permanently undergo events of folding, unfolding, and refolding.

4 Methods

4.1 Cloning

The sequence coding for YAP residues 50-171 was cloned into a pETM14 vector by Sequence and Ligation Independent Cloning (SLIC) (Scholz et al. 2013). Therefore, the coding sequence of YAP was amplified by polymerase chain reaction (PCR) using primers containing 25 bp overlapping homologies of the target vector at each end. The remaining copies of the initial template vector were removed by a one-hour digest with the restriction enzyme DPNI. An aliquot of approximately 100 ng of the PCR product (coding sequence of YAP 50-171) was mixed in a total volume of 10 µl with approximately 100 ng of the target pETM14 vector and recA; consequently, the mixture was incubated at 37°C for an additional hour. The recombinase recA recombines the PCR products into the target vector due to the overlapping homologous regions. The whole 10 µl were transformed into *E. coli* TOP10 cells and the resulting plasmids were evaluated by sequencing. The final pETM14 vector contained a YAP fusion protein with His6-tag and a 3 C protease cleavage site at the N-terminus (see Fig. 4-1).

4.2 Site-Directed Mutagenesis

The introduction of a MTSL spin-label (see section 4.4) requires a Cysteine to covalently attach itself. Therefore, three different mutants were produced by site-directed mutagenesis

via PCR. Two insertions (on the N- and the C-terminus) and one mutation of S103 to C103 were carried out. For PCR-mediated mutagenesis, a single PCR step using full plasmid amplification was used (Carey et al. 2013). Hence, 0.2 µl of each 25 bp primer (concentration of 100 µM), 50 ng of plasmid DNA and 20 µl Phusion Flash PCR Master Mix (Thermo Fisher) were combined in a total volume of 40 µl. Then PCR was run for 20 cycles, each consisting of 30 seconds of denaturation at 96 °C and of 2 minutes of elongation at 72 °C. The remaining copies of the initial template vector were removed by a one-hour digest with the restriction enzyme DPNI. Afterwards, 2 µl of each PCR product were transformed into *E. coli* TOP10 cells and the resulting plasmids were evaluated by sequencing.
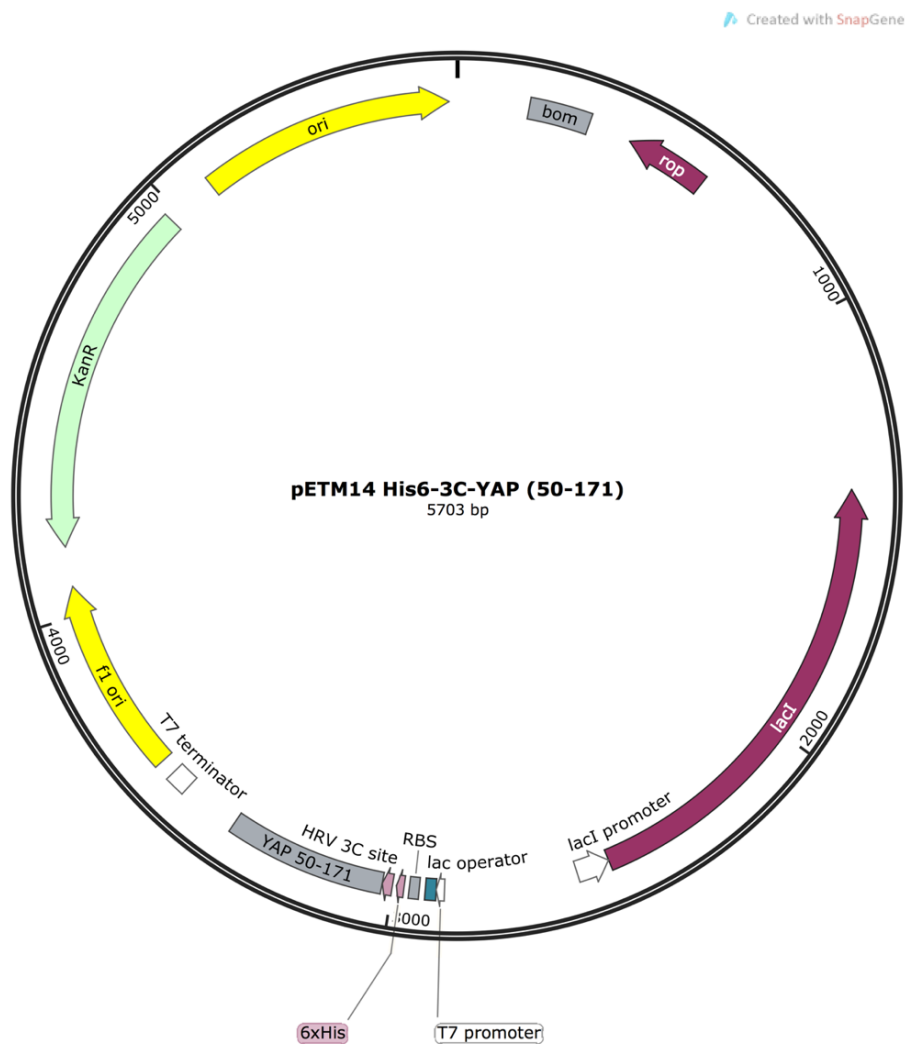

Fig. 4-1: Map of the Plasmid pETM14 His6-3C-YAP (50-171) produced by SLIC and used for expression.

4.3 Protein Expression and Purification

4.3.1 YAP

The plasmid, containing the fusion protein with a His6-tag at the N-terminus and a 3C protease cleavage site (see section 4.1), was transformed into *Escherichia coli* Tuner™(DE3). Four liters of LB medium, supplemented with Kanamycin, were inoculated with the overnight culture and incubated at 37 °C until an OD_{600} of 0.8. The cells were centrifuged and all the pellets were combined and resuspended in one liter of M9 minimal medium containing 1 g/L ^{15}N ammonium chloride (Sigma Aldrich) and 3 g/L ^{13}C glucose (Cambridge Isotope) as the sole source of nitrogen and carbon, respectively (Marley et al. 2001). After an additional hour at 37 °C, the expression was induced with the addition of 0.8 mM IPTG and cells were incubated for 18 hours at 30 °C and consecutively harvested by centrifugation and stored at -20 °C.

Frozen cell pellets were resuspended in lysis buffer (20 mM Tris, 150 mM NaCl, 30 mM Imidazole, pH 7.8), supplemented with 50 µl of Protease Inhibitor Cocktail (Thermo Scientific), and lysed by sonication on ice. The lysate was clarified by centrifugation and the supernatant was loaded onto a HisTrap FF column and washed with 8 column volumes of wash buffer (20 mM Tris, 150 mM NaCl, 40 mM Imidazole, pH 7.8). After eluting with 15 ml of elution buffer (20 mM Tris, 150 mM NaCl, 300 mM Imidazole, 1 mM EDTA, pH 7.8), the eluate was concentrated to 2 ml and dialyzed overnight against an excess of NMR buffer (20 mM BisTris, 150 mM NaCl, 1 mM EDTA, pH 6.0). Consequently, the His6-tag was removed by 3C protease cleavage overnight at 4 °C. NaCl was added to the final concentration of 1 M and the solution was heated to 90 °C for 10 min. After centrifugation, the supernatant was loaded onto a HiLoad 16/600 (GE Healthcare) size exclusion column, equilibrated with the NMR buffer. Fractions between 61 and 69 ml (see Fig 4-3) were pooled and concentrated. In the case of the Cysteine mutants, all the buffers were supplemented with 1 mM DTT.

Purified protein, which was >95% pure as assessed by SDS/PAGE (see Fig 4-2), was concentrated to approximately 0.5 mM in the NMR buffer containing 10% D_2O. Owing to the lack of absorbance at 280 nm, the protein concentration was determined by the Pierce BCA Protein Assay (Thermo Scientific).
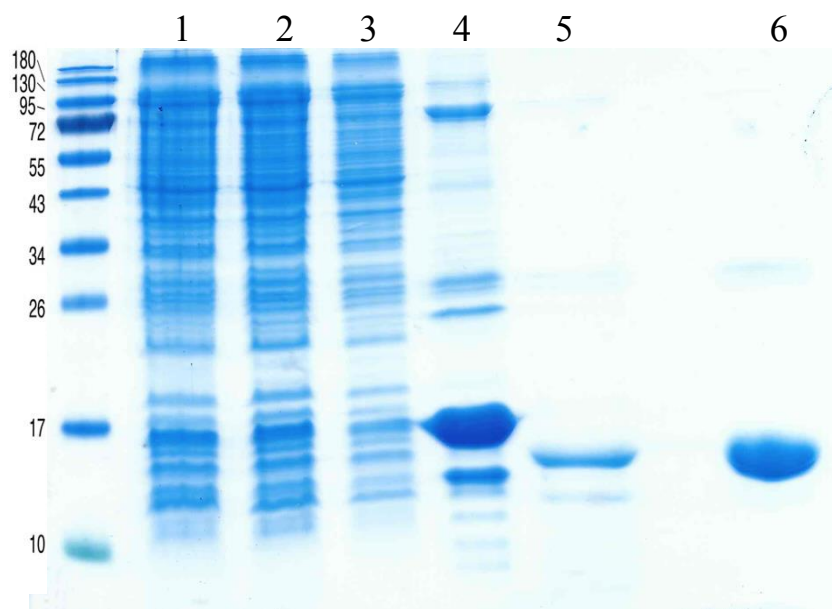
Fig. 4-2: SDS/PAGE Gel of YAP purification. (1) Complete Lysate; (2) Supernatant after Centrifugation; (3) HisTrap Flow-through; (4) Concentrated HisTrap Elute; (5) Post 3 C Protease Digest; and (6) Final Sample.
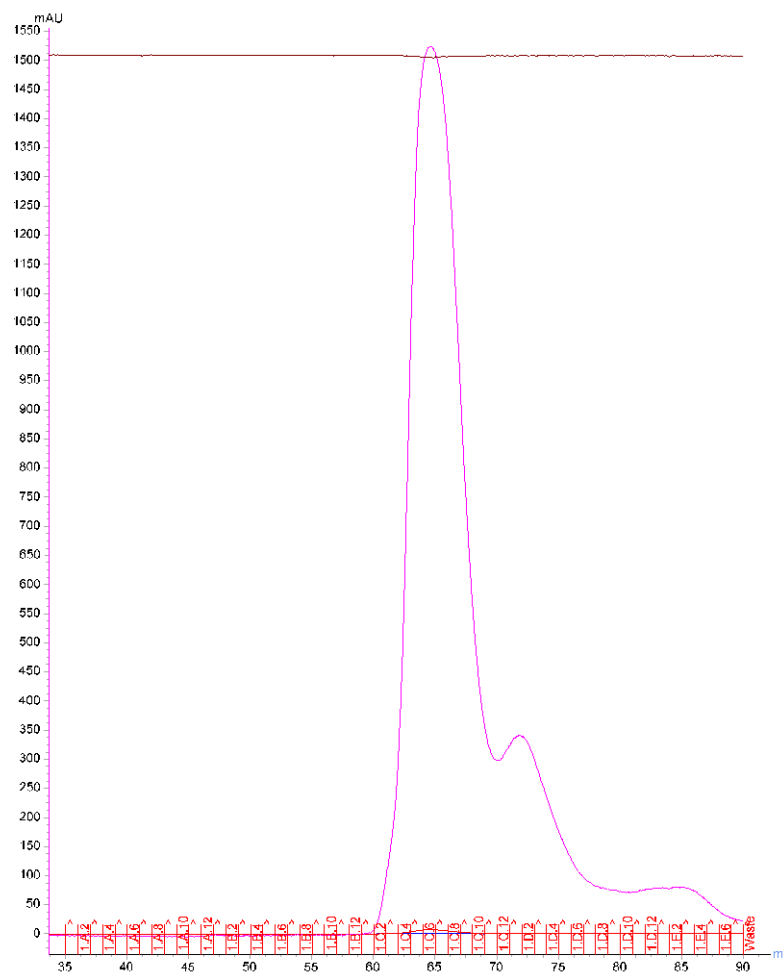

Fig. 4-3: Chromatogram of YAP purification on the size exclusion column HiLoad 16/600 (GE Healthcare).

4.3.2 TEAD4

Used C-terminal YAP binding domain of the TEAD4 protein was kindly provided by Novartis Institutes for Biomedical Research.

4.4 MTSL Tagging

The MTSL tagging was initiated combining 1 ml of protein solution (see section 4.3.1) with 1 ml of MTSL reaction buffer (100 mM NaP, 1 mM EDTA, pH 8.0) and by incubating it at RT for 15 min after the addition of a 10-fold excess (in comparison to the protein concentration) of DTT. This ensures that all the Cysteines are reduced for the MTSL-tagging procedure. Afterwards, DTT was removed by the PD-10 desalting column and the protein solution was eluted in 3.3 ml of MTSL reaction buffer. From a 50 mM DMSO stock solution, two times excess of MTSL was added to the protein solution. Consequently, the protein solution containing MTSL was incubated for 3 h at 30 °C with agitation. Finally, the free MTSL was removed and the sample concentrated by exchange with the NMR Buffer via a Amicon Centricon MWCO 3 kDa. For the measurement of the diamagnetic control experiments, the free electron of the MTSL tag was reduced by a two-fold excess of ascorbic acid.

4.5 NMR Spectroscopy

NMR experiments were performed at 298 K using a Bruker Avance III 800 MHz, Bruker Neo 600 MHz, and Bruker Neo 500 MHz spectrometer. Data were processed using NMRPipe (Delaglio et al. 1995) and spectra were analyzed using CcpNmr (Vranken et al. 2005) and Sparky (Goddard and Kneller 2004). Further data analysis and plots were performed and created, respectively, with RStudio (RStudio Team 2017).

4.6 Mass Spectrometry

Liquid chromatography-mass spectrometry (LC-MS) experiments were carried out by the MFPL Mass Spectrometry Service Facility. The YAP sample was diluted with H_2O to a concentration of approximately 10 ng/µl, resulting in approximately 60 ng of protein on the column. The average masses were reconstructed with MaxEnt1 (Cottrell and Green 1998).

6 References

Carey MF, Peterson CL, Smale ST (2013) PCR-mediated site-directed mutagenesis. Cold Spring Harb Protoc 2013:738–742. doi: 10.1101/pdb.prot076505

Cavanagh J, Fairbrother WJ, Palmer AG, et al (2007) Protein NMR Spectroscopy. Principles and Practice, 2nd Editio. Elsevier Inc., London

Clore GM (2015) Practical Aspects of Paramagnetic Relaxation Enhancement in Biological Macromolecules, 1st edn. Elsevier Inc.

Cottrell JC, Green BN (1998) MaxEnt : An Essential Maximum Entropy Based Tool for Interpreting Multiply-Charged Electrospray Data.

Danielsson J, Liljedahl L, Bárány-Wallje E, et al (2008) The intrinsically disordered RNR inhibitor Sml1 is a dynamic dimer. Biochemistry 47:13428–13437. doi: 10.1021/bi801040b

Delaglio F, Grzesiek S, Vuister GW, et al (1995) NMRPipe: A multidimensional spectral processing system based on UNIX pipes. J Biomol NMR 6:277–293. doi: 10.1007/BF00197809

Dunker AK, Cortese MS, Romero P, et al (2005) Flexible nets The roles of intrinsic disorder in protein interaction networks. FEBS J 272:5129–5148. doi: 10.1111/j.1742-4658.2005.04948.x

Fischer E (1894) Einfluss der Configuration auf die Wirkung der Enzyme. Berichte der Dtsch Chem Gesellschaft 27:2985–2993. doi: 10.1002/cber.18940270364

Goddard Td, Kneller DG (2004) SPARKY 3. Univ California, San Fr 14:15.

Halder G, Johnson RL (2011) Hippo signaling: growth control and beyond. Development 138:9–22. doi: 10.1242/dev.045500

Hammes GG, Chang Y-C, Oas TG (2009) Conformational selection or induced fit: A flux description of reaction mechanism. Proc Natl Acad Sci 106:13737–13741. doi: 10.1073/pnas.0907195106

Hau JC, Erdmann D, Mesrouze Y, et al (2013) The TEAD4-YAP/TAZ Protein-Protein Interaction: Expected Similarities and Unexpected Differences. ChemBioChem 14:1218–1225.

Iakoucheva LM, Brown CJ, Lawson JD, Dunker AK (2002) Intrinsic Disorder in Cell-signaling and Cancer-associated Proteins. J Mol Biol 323:573–584. doi: 10.1016/S0022-2836(02)00969-5

Jensen MR, Ruigrok RWH, Blackledge M (2013) Describing intrinsically disordered proteins at atomic resolution by NMR. Curr Opin Struct Biol 23:426–435. doi: 10.1016/j.sbi.2013.02.007

Kay LE, Torchia DA, Bax A (1989) Backbone Dynamics of Proteins As Studied by 15N Inverse Detected Heteronuclear NMR Spectroscopy: Application to Staphylococcal Nuclease. Biochemistry 28:8972–8979. doi: 10.1021/bi00449a003

Kjaergaard M, Poulsen FM (2012) Disordered proteins studied by chemical shifts. Prog Nucl Magn Reson Spectrosc 60:42–51. doi: 10.1016/j.pnmrs.2011.10.001

Kneller JM, Lu M, Bracken C (2002) An effective method for the discrimination of motional anisotropy and chemical exchange. J Am Chem Soc 124:1852–1853. doi: 10.1021/ja017461k

Konrat R (2015) IDPs: Less Disordered and More Ordered than Expected. Biophys J 109:1309–1311. doi: 10.1016/j.bpj.2015.06.041

Konrat R (2014) NMR contributions to structural dynamics studies of intrinsically disordered proteins. J Magn Reson 241:74–85. doi: 10.1016/j.jmr.2013.11.011

Konrat R (2009) The protein meta-structure: A novel concept for chemical and molecular biology. Cell Mol Life Sci 66:3625–3639. doi: 10.1007/s00018-009-0117-0

Kosen PA (1989) Spin labeling of proteins. Methods Enzymol 177:86–121. doi: 10.1016/0076-6879(89)77007-5

Koshland DE (1958) Application of a Theory of Enzyme Specificity to Protein Synthesis. Proc Natl Acad Sci 44:98–104. doi: 10.1073/pnas.44.2.98

Levitt M. (2008) Spin Dynamics: Basics of Nuclear Magnetic Resonance, Second edi. John Wiley & Sons Ltd., Chichester

Li Z, Zhao B, Wang P, et al (2010) Structural insights into the YAP and TEAD complex service Structural insights into the YAP and TEAD complex. Genes Dev 235–240. doi: 10.1101/gad.1865810

Lichtenecker RJ, Weinhäupl K, Schmid W, Konrat R (2013) α-Ketoacids as precursors for phenylalanine and tyrosine labelling in cell-based protein overexpression. J Biomol NMR 57:327–331. doi: 10.1007/s10858-013-9796-9

Lipari G, Szabo A (1982) Model-Free Approach to the Interpretation of Nuclear Magnetic Resonance Relaxation in Macromolecules. 1. Theory and Range of Validity. J Am Chem Soc 104:4546–4559. doi: 10.1021/ja00381a009

Liu AM, Wong KF, Jiang X, et al (2012) Regulators of mammalian Hippo pathway in cancer. Biochim Biophys Acta - Rev Cancer 1826:357–364. doi: 10.1016/j.bbcan.2012.05.006

Ma Y, Yang Y, Wang F, et al (2015) Hippo-YAP signaling pathway: A new paradigm for cancer therapy. Int J Cancer 137:2275–2286. doi: 10.1002/ijc.29073

Marion D, Driscoll PC, Kay LE, et al (1989) Overcoming the Overlap Problem in the Assignment of 1H NMR Spectra of Larger Proteins by Use of Three-Dimensional Heteronuclear 1H-15N Hartmann-Hahn-Multiple Quantum Coherence and Nuclear Overhauser-Multiple Quantum Coherence Spectroscopy: Application to . Biochemistry 28:6150–6156. doi: 10.1021/bi00441a004

Marley J, Lu M, Bracken C (2001) A method for efficient isotopic labeling of recombinant proteins. J Biomol NMR 20:71–75. doi: 10.1023/A:1011254402785

Marsh J a, Singh VK, Jia Z, Forman-Kay JD (2006) Sensitivity of secondary structure propensities to sequence differences between alpha- and gamma-synuclein: implications for fibrillation. Protein Sci 15:2795–2804. doi: 10.1110/ps.062465306

Mesrouze Y, Bokhovchuk F, Meyerhofer M, et al (2017) Dissection of the interaction between the intrinsically disordered YAP protein and the transcription factor TEAD. Elife 6:1–16. doi: 10.7554/eLife.25068.001

Metallo SJ (2010) Intrinsically disordered proteins are potential drug targets. Curr Opin Chem Biol 14:481–488. doi: 10.1016/j.cbpa.2010.06.169

Oldfield CJ, Dunker AK (2014) Intrinsically Disordered Proteins and Intrinsically Disordered Protein Regions. Annu Rev Biochem 83:553–584. doi: 10.1146/annurev-biochem-072711-164947

Pobbati A V., Han X, Hung AW, et al (2015) Targeting the Central Pocket in Human Transcription Factor TEAD as a Potential Cancer Therapeutic Strategy. Structure 23:2076–2086. doi: 10.1016/j.str.2015.09.009

Pobbati A V., Hong W (2013) Emerging roles of TEAD transcription factors and its coactivators in cancers. Cancer Biol Ther 14:390–398. doi: 10.4161/cbt.23788

Reddy T, Rainey JK (2010) Interpretation of biomolecular NMR spin relaxation parameters. Biochem Cell Biol 88:131–142. doi: 10.1139/O09-182

RStudio Team - (2017) RStudio: Integrated Development for R. [Online] RStudio, Inc, Boston, MA URL http//www rstudio com RStudio, Inc., Boston, MA. doi: 10.1007/978-81-322-2340-5

Santucci M, Vignudelli T, Ferrari S, et al (2015) The Hippo Pathway and YAP/TAZ-TEAD Protein-Protein Interaction as Targets for Regenerative Medicine and Cancer Treatment. J Med Chem 58:4857–4873. doi: 10.1021/jm501615v

Scholz J, Besir H, Strasser C, Suppmann S (2013) A new method to customize protein expression vectors for fast, efficient and background free parallel cloning. BMC Biotechnol 13:12. doi: 10.1186/1472-6750-13-12

Solyom Z, Schwarten M, Geist L, et al (2013) BEST-TROSY experiments for time-efficient sequential resonance assignment of large disordered proteins. J Biomol NMR 55:311–321. doi: 10.1007/s10858-013-9715-0

Staley BK, Irvine KD (2012) Hippo signaling in Drosophila: Recent advances and insights. Dev Dyn 241:3–15. doi: 10.1002/dvdy.22723

Tollinger M, Skrynnikov NR, Mulder FAA, et al (2001) Slow dynamics in folded and unfolded states of an SH3 domain. J Am Chem Soc 123:11341–11352. doi: 10.1021/ja011300z

Tompa P (2011) Unstructural biology coming of age. Curr Opin Struct Biol 21:419–425. doi: 10.1016/j.sbi.2011.03.012

Tompa P (2010) Structure and Function of Intrinsically Disordered Proteins. CRC Press, Boca Raton; London; New York

Tremblay AM, Camargo FD (2012) Hippo signaling in mammalian stem cells. Semin Cell

Dev Biol 23:818–826. doi: 10.1016/j.semcdb.2012.08.001

Tsai C-J, Ma B, Nussinov R (1999) Folding and binding cascades: Shifts in energy landscapes. Proc Natl Acad Sci 96:9970–9972. doi: 10.1073/pnas.96.18.9970

Uversky VN (2011) Intrinsically disordered proteins from A to Z. Int J Biochem Cell Biol 43:1090–1103. doi: 10.1016/j.biocel.2011.04.001

Uversky VN (2014) Introduction to intrinsically disordered proteins (IDPs). Chem Rev 114:6557–6560. doi: 10.1021/cr500288y

Vassilev A, Kaneko KJ, Shu H, et al (2001) YAP65 , a Src / Yes-associated protein localized in the cytoplasm TEAD / TEF transcription factors utilize the activation domain of YAP65 , a Src / Yes-associated protein localized in the cytoplasm. Genes Dev 15:1229–1241. doi: 10.1101/gad.888601

Vranken WF, Boucher W, Stevens TJ, et al (2005) The CCPN data model for NMR spectroscopy: Development of a software pipeline. Proteins Struct Funct Genet 59:687–696. doi: 10.1002/prot.20449

Wright PE, Dyson HJ (1999) Intrinsically unstructured proteins: re-assessing the protein structure-function paradigm. J Mol Biol 293:321–331. doi: 10.1006/jmbi.1999.3110

Zhang K, Qi HX, Hu ZM, et al (2015) YAP and TAZ Take Center Stage in Cancer. Biochemistry 54:6555–6566. doi: 10.1021/acs.biochem.5b01014

Zhang Z, Lin Z, Zhou Z, et al (2014) Structure-based design and synthesis of potent cyclic peptides inhibiting the YAP-TEAD protein-protein interaction. ACS Med Chem Lett 5:993–998. doi: 10.1021/ml500160m

Zhao B, Li L, Tumaneng K, et al (2010) A coordinated phosphorylation by Lats and CK1 regulates YAP stability through SCFβ-TRCP. Genes Dev 24:72–85. doi: 10.1101/gad.1843810

Zhao B, Tumaneng K, Guan KL (2011) The Hippo pathway in organ size control, tissue regeneration and stem cell self-renewal. Nat Cell Biol 13:877–883. doi: 10.1038/ncb2303

Zhao B, Zhao B, Wei X, et al (2007) Inactivation of YAP oncoprotein by the Hippo pathway is involved in cell contact inhibition and tissue growth control. Genes Dev 21:2747–

2761. doi: 10.1101/gad.1602907.Hpo/Sav

Zuiderweg ERP, Fesik SW (1989) Heteronuclear Three-Dimensional NMR Spectroscopy of the Inflammatory Protein C5a. Biochemistry 28:2387–2391. doi: 10.1021/bi00432a008